

J80-227

# Harmonic Linearization Method for High-Intensity Sound in Two-Dimensional Lined Ducts

Morgan S. Tsai\*

Boeing Commercial Airplane Co., Seattle, Wash.

The harmonic linearization method is used to calculate the attenuation of the high-intensity sound in two-dimensional ducts of uniform cross section. The complex wave number in the transcendental equation is analytically expressed in terms of lining properties and sound pressure. Very good agreements between the calculated results and experimental data are obtained. When the linear resistivity and the thickness of the porous face-sheet decrease, the bandwidth of the adverse nonlinear effect becomes narrower and the frequencies corresponding to this bandwidth shift to higher frequencies.

## I. Introduction

THE products of acoustic quantities are omitted in the linear acoustic problem. The omission of the nonlinear acoustic products is not tolerated for analyzing the propagation and attenuation of high-intensity sound in lined ducts. The first kind of nonlinear acoustic products is contributed by the acoustic properties of the lining material. Impedance measurements of typical linings indicate that the acoustic resistance consists of two components: 1) linear viscous resistance, which depends only on the characteristics of the lining material; and 2) nonlinear resistance, which depends on both the characteristics of the lining material and the normal acoustic velocity. The inclusion of the second components of the acoustic resistance in the governing equation of motion for the flow in the porous medium produces the nonlinear acoustic products which will result in the recreation of the fundamental harmonic. Similarly, the inclusion of the second kind of the nonlinear acoustic products, the gas nonlinearity, in the unsteady Euler equation for the flow in the duct and the cavities will also result in the recreation of the fundamental harmonic.

The nonlinear attenuations of high-intensity sound in lined ducts have been calculated by using the one-dimensional transmission-line approximation,<sup>1</sup> the finite-difference approximation,<sup>2</sup> and the method of multiple scales.<sup>3,4</sup> When the sound pressure level is near or above 160 dB, the uniform perturbation expansion technique does not give good prediction, which is attributed to the strong interactions between the fundamental harmonic and its higher harmonics. These interactions will recreate a fundamental harmonic of which the order of magnitude is almost the same as that of the original fundamental harmonic. The eigenvalue in the transcendental equation has to correspond to all the waves of the same harmonic with the same order of magnitude, and the wave number becomes acoustic pressure dependent.

The recreation of the fundamental harmonic due to the nonlinearity suggests the use of the harmonic linearization method<sup>5,6</sup> to obtain the dependence of the eigenvalue, wave number, and attenuation on the acoustic pressure. Thus, the purpose of this paper is to use the harmonic linearization method to calculate the attenuation of high-density sound in a two-dimensional duct lined with a point-reacting acoustic material consisting of a porous face-sheet followed by honeycomb cavities and backed by the impervious wall of the

duct. The waves in the duct are coupled with those in the porous face-sheet and the cavities by using the continuities of particle velocity and pressure at the interfaces between the plate and the duct or cavities.

## II. Problem Formulation

Let us consider high-intensity sound propagating in uniform ducts whose walls are lined with nonlinear acoustic materials. The sound is assumed to propagate into an inviscid and irrotational gas at rest having a uniform pressure  $p_0^*$  and a uniform density  $\rho_0^*$ . A Cartesian coordinate system is introduced such that the  $x$  axis is parallel to the duct axis. The half-width of the duct  $d^*$ , the ambient speed of sound  $C_0^*$ , and  $\rho_0^*$  are used as reference quantities to nondimensionalize physical quantities, letting starred and unstarred quantities denote, respectively, dimensional and dimensionless quantities.

Based on the foregoing assumptions, the governing equations for the flow in the duct are

$$\frac{\partial^2 \phi}{\partial x^2} + \frac{\partial^2 \phi}{\partial y^2} - \frac{\partial^2 \phi}{\partial t^2} = 2 \frac{\partial \phi}{\partial x} \frac{\partial \phi}{\partial y} \frac{\partial^2 \phi}{\partial x \partial y} + \frac{\partial}{\partial t} \left[ \left( \frac{\partial \phi}{\partial x} \right)^2 + \left( \frac{\partial \phi}{\partial y} \right)^2 \right] + \frac{\partial^2 \phi}{\partial x^2} \left( \frac{\partial \phi}{\partial x} \right)^2 - \left( \frac{\partial^2 \phi}{\partial x^2} + \frac{\partial^2 \phi}{\partial y^2} \right) \times (1 - \gamma) \left[ \frac{\partial \phi}{\partial t} + \frac{1}{2} \left( \frac{\partial \phi}{\partial y} \right)^2 + \frac{1}{2} \left( \frac{\partial \phi}{\partial x} \right)^2 \right] + \frac{\partial^2 \phi}{\partial y^2} \left( \frac{\partial \phi}{\partial y} \right)^2 \equiv N_1 \quad (1)$$

and

$$P - \frac{1}{\gamma} + \frac{\partial \phi}{\partial t} = \frac{1}{2} \left( \frac{\partial \phi}{\partial t} \right)^2 - \frac{1}{2} (\nabla \phi)^2 \left( 1 - \frac{\partial \phi}{\partial t} \right) - \frac{2 - \gamma}{6} \left( \frac{\partial \phi}{\partial t} \right)^3 + O(\phi^4) \equiv N_2 \quad (2)$$

where  $\phi$  is the velocity potential and  $\gamma$  the specific heat ratio.

The cross-sectional dimensions of the cellular cavities are small relative the acoustic wavelength of interest. The equations describing the velocity potential  $\Phi$  and the pressure  $P_c$  in the cavities are

$$\frac{\partial^2 \Phi}{\partial y^2} - \frac{\partial^2 \Phi}{\partial t^2} = -(1 - \gamma) \left[ \frac{\partial \Phi}{\partial t} + \frac{1}{2} \left( \frac{\partial \Phi}{\partial y} \right)^2 \right] \frac{\partial^2 \Phi}{\partial y^2} + 2 \frac{\partial \Phi}{\partial y} \frac{\partial^2 \Phi}{\partial y \partial t} + \frac{\partial^2 \Phi}{\partial y^2} \left( \frac{\partial \Phi}{\partial y} \right)^2 \equiv N_3 \quad (3)$$

Presented as Paper 79-0621 at the AIAA 5th Aeroacoustics Conference, Seattle, Wash., March 12-14, 1979; submitted April 9, 1979; revision received March 4, 1980. Copyright © American Institute of Aeronautics and Astronautics, Inc., 1979. All rights reserved.

Index categories: Aeroacoustics; Aerodynamics; Noise.

\*Specialist Engineer, Member AIAA.

00001  
00023  
20001

and

$$P_c - \frac{1}{\gamma} + \frac{\partial \Phi}{\partial t} = \frac{1}{2} \left( \frac{\partial \Phi}{\partial t} \right)^2 - \frac{1}{2} \left( \frac{\partial \Phi}{\partial y} \right)^2 \left( 1 - \frac{\partial \Phi}{\partial t} \right) - \frac{2-\gamma}{6} \left( \frac{\partial \Phi}{\partial t} \right)^3 + O(\Phi)^4 \equiv N_4 \quad (4)$$

When the sound pressure level (SPL) is higher than 130 dB, the resistivity increases with increasing particle velocity. Following Green and Dawez<sup>7</sup> and Irmay,<sup>8</sup> we let

$$\sigma = \sigma_0 + \sigma_1 |v| \quad (5)$$

where  $\sigma_0$  is the linear term (viscous) and  $\sigma_1 |v|$  is the nonlinear term due to the inertia effect. The porous sheet is assumed to be homogeneous and rigid medium. Its thickness  $b$  is very small compared with the wavelength of interest, so that waves can be considered to propagate only in the direction normal to the porous sheet. The governing equations within the porous material, given by Morse and Ingard,<sup>9</sup> are as follows:

$$\Omega \frac{\partial \rho}{\partial t} + \frac{\partial}{\partial y} (\rho v) = 0 \quad (6)$$

$$\rho_e \frac{\partial v}{\partial t} + \sigma_0 v + \frac{\partial P}{\partial y} = -\sigma_1 v |v| \equiv N_5 \quad (7)$$

and

$$\gamma P_p = \rho^n \quad (8)$$

where  $n$  is generally a complex number which has been discussed in Ref. 9,  $v$  is the velocity in the  $y$  direction,  $\Omega$  is the material porosity,  $\rho$  and  $P_p$  are the gas density and pressure, respectively,  $\rho_e = S\rho/\Omega$  is the dimensionless effective density,  $S$  is the structure factor, and  $\sigma = \sigma^* d^*/\rho_0^* C_0^*$  is the dimensionless resistivity. Both Zwikker and Kosten<sup>10</sup> and Morse and Ingard<sup>9</sup> pointed out that the increases of effective density are due to the constrictive passages of fluid particles, so the value of  $S$  is usually greater than unity. Eliminating  $P_p$  and  $\rho$  among Eqs. (6-8) gives

$$S \frac{\partial^2 v}{\partial t^2} - \frac{\eta}{\gamma} \frac{\partial^2 v}{\partial y^2} + \Omega \sigma_0 \frac{\partial v}{\partial t} = -\sigma_1 \Omega \left( v \frac{\partial |v|}{\partial t} + |v| \frac{\partial v}{\partial t} \right) \equiv N_6 \quad (9)$$

Kurze and Allen<sup>2</sup> indicated that if the "equivalent SPL" generated by the turbulent flow over the solid and porous surfaces exceeds the SPL difference across the resistive material, then the resistivity is independent of duct flow velocity. Dean<sup>11</sup> and Hersh and Walker<sup>12</sup> also bound the negligible effects of grazing flow on resistivity for certain types of lining such as the fiber-metal liner. For a given duct lining, whether the effect of flow will linearize the attenuation along the duct needs further investigation. The present study is limited to consider no mean flow.

Although there is no mean flow, the axial component of the acoustic velocity can be discontinuous in the immediate neighborhood of the interface, which separate the inviscid irrotational flows in the duct and cavities from the flowfield in the porous sheet. The fluid particles initially located on the interface will always remain on the interfaces which are fluctuating about their undisturbed positions at  $y=1$  and  $y=1+b$ , respectively. Let  $y=1+\eta(x,t)$  and  $y=1+b+\zeta(x,t)$  be the locations of these interfaces. Then the balance of normal forces at the interfaces give

$$P_p - P = -\eta \frac{\partial P_p}{\partial y} - \frac{\eta}{2} \frac{\partial^2 P_p}{\partial y^2} + \eta \frac{\partial P}{\partial y} + \frac{\eta^2}{2} \frac{\partial^2 P}{\partial y^2} \equiv N_7 \text{ at } y=1 \quad (10)$$

$$P_p - P_c = -\zeta \frac{\partial P_p}{\partial y} - \frac{\zeta^2}{2} \frac{\partial^2 P_p}{\partial y^2} + \zeta \frac{\partial P_c}{\partial y} + \frac{\zeta^2}{2} \frac{\partial^2 P_c}{\partial y^2} \equiv N_8 \text{ at } y=1+b \quad (11)$$

The substantial derivatives of  $(y=1+\eta)$  and  $(y=1+b+\zeta)$  result in

$$\frac{\partial \eta}{\partial t} - \frac{\partial \phi}{\partial y} = \eta \frac{\partial^2 \phi}{\partial y^2} + \frac{\eta^2}{2} \frac{\partial^3 \phi}{\partial y^3} - \left( \frac{\partial \phi}{\partial x} + \eta \frac{\partial^2 \phi}{\partial x \partial y} \right) \frac{\partial \eta}{\partial x} \equiv N_9 \text{ at } y=1 \quad (12)$$

$$\frac{\partial \eta}{\partial t} - v = \eta \frac{\partial v}{\partial y} + \frac{\eta^2}{2} \frac{\partial^2 v}{\partial y^2} \equiv N_{10} \text{ at } y=1 \quad (13)$$

$$\frac{\partial \zeta}{\partial t} - \frac{\partial \Phi}{\partial y} = \zeta \frac{\partial^2 \Phi}{\partial y^2} + \frac{\zeta^2}{2} \frac{\partial^3 \Phi}{\partial y^3} \equiv N_{11} \text{ at } y=1+b \quad (14)$$

$$\frac{\partial \zeta}{\partial t} - v = \zeta \frac{\partial v}{\partial y} + \frac{\zeta^2}{2} \frac{\partial^2 v}{\partial y^2} \equiv N_{12} \text{ at } y=1+b \quad (15)$$

Note that Eqs. (10-15) were obtained after transferring the boundary conditions from  $y=1+b+\zeta$  and  $y=1+\eta$  to  $y=1+b$  and  $y=1$ , respectively. The detailed derivations for Eqs. (1-4) and (9-15) were given in Ref. 13.

The symmetric disturbance mode requires that

$$\frac{\partial \phi}{\partial y} = 0 \text{ at } y=0 \quad (16)$$

The requirement that the velocity in the cavity vanishes at the impervious wall yields

$$\frac{\partial \Phi}{\partial y} = 0 \text{ at } y=1+b+h \quad (17)$$

where  $h$  is the dimensionless cavity depth.

### III. Solutions

The waves of finite amplitude propagating in the lined duct are dispersive. Except for the harmonic resonance, we are able to treat a single-frequency wave individually. When the nonlinear terms  $N_i$  become zero, the linear solutions are of the forms

$$\phi_0 = A \cos \kappa_0 y e^{i\theta - \alpha_0 x} + CC = a_1 \cos(\theta + \tau_1) \quad (18)$$

$$\Phi_0 = B \cos [\omega(y-1-b-h)] e^{i\theta - \alpha_0 x} + CC = a_2 \cos(\theta + \tau_2) \quad (19)$$

$$v_0 = C \cos [\kappa_{p0}(y+\Psi)] e^{i\theta - \alpha_0 x} + CC = a_3 \cos(\theta + \tau_3) \quad (20)$$

where CC stands for complex conjugate and

$$\kappa_0^2 = \omega^2 - k_0^2 = \omega^2 - (k_r + i\alpha_0)^2 \quad (21)$$

$$\kappa_{p0}^2 = \frac{\gamma\omega}{n} (\omega S + i\Omega\sigma_0) \quad (22)$$

$$\theta = k_r x - \omega t \quad (23)$$

The complex amplitudes  $A$ ,  $B$ , and  $C$  are constants in linear system, whereas they become functions of time and spatial distance in the nonlinear system. Their dependences on  $t$  and  $x$  through  $\theta$  can be found by the Van der Pol<sup>14</sup> method as

$$\frac{dA}{d\theta} = \frac{N_1 e^{-i\theta + \alpha_0 x}}{i(k_0^2 + \bar{k}_0^2 - 2\omega^2) \cos \kappa_0 y} \quad (24)$$

$$\frac{dB}{d\theta} = \frac{N_3 e^{-i\theta + \alpha_0 x}}{-2i\omega^2 \cos[\omega(y-l-b-h)]} \quad (25)$$

$$\frac{dC}{d\theta} = \frac{N_6 e^{-i\theta + \alpha_0 x}}{2i\omega^2 \text{Scos}[\kappa_{p0}(y+\Psi)]} \quad (26)$$

The magnitudes of the nonlinearity  $N_1$ ,  $N_3$ , and  $N_6$  are of order  $|Ae^{-\alpha_0 x}|^2$ ,  $|Be^{-\alpha_0 x}|^2$  and  $|Ce^{-\alpha_0 x}|^2$ , respectively. As the acoustic velocity is less than the speed of sound, the dimensionless complex amplitudes  $A$ ,  $B$ , and  $C$  are less than unity. Equations (24-26) indicated that the variations of the complex amplitudes with  $\theta$  are much less than unity. Thus,  $A$ ,  $B$ , and  $C$  are slowly varying functions of  $\theta$ , i.e., the amplitude and phase of the acoustic velocities hardly change when  $\theta$  varies from 0 to  $2\pi$ .

Expanding all of the foregoing nonlinear terms  $N_j$  in Fourier series, we get

$$N_j = M_j e^{i\theta - \alpha x} + CC + \text{Harmonic other than } \theta \quad (27)$$

where

$$M_j = \frac{1}{2\pi} \int_0^{2\pi} N_j e^{-i\theta + \alpha x} d\theta \quad (28)$$

The expressions for  $M_j$  are shown in the Appendix. The slowly varying functions  $A$ ,  $B$ , and  $C$  in the integral of Eq. (28) are treated as constants when  $\theta$  varies over  $(0, 2\pi)$ . In the harmonic linearization methods, only the terms involved with the harmonic  $\theta$  are considered and Eq. (27) can be approximated as

$$N_j = E_j \cos(\theta + \tau_j) + F_j \sin(\theta + \tau_j) = \mathcal{L}_j(U) \quad (29)$$

where

$$\mathcal{L}_j \equiv E_j + \frac{F_j}{\omega} \frac{\partial}{\partial t} \quad (30)$$

$\tau_j$  is chosen as one of the phase angles  $\tau_1, \tau_2, \tau_3$  shown in Eqs. (18-20). Similarly,  $U$  is chosen as one of the expressions  $\phi/a_1$ ,  $\Phi/a_2$ , and  $v/a_3$ . Substituting Eqs. (29) and (30) into Eqs. (1-4), (7), and (9-15) gives a set of equivalent linear equations as follows:

$$\frac{\partial^2 \phi}{\partial x^2} + \frac{\partial^2 \phi}{\partial y^2} - \frac{\partial^2 \phi}{\partial t^2} - \mathcal{L}_1\left(\frac{\phi}{a_1}\right) = 0 \quad (31)$$

$$P - \frac{1}{\gamma} + \frac{\partial \phi}{\partial t} - \mathcal{L}_2\left(\frac{\phi}{a_1}\right) = 0 \quad (32)$$

$$\frac{\partial^2 \Phi}{\partial y^2} - \frac{\partial^2 \Phi}{\partial t^2} - \mathcal{L}_3\left(\frac{\Phi}{a_2}\right) = 0 \quad (33)$$

$$P_c - \frac{1}{\gamma} + \frac{\partial \Phi}{\partial t} - \mathcal{L}_4\left(\frac{\Phi}{a_2}\right) = 0 \quad (34)$$

$$\rho_e \frac{\partial v}{\partial t} + \sigma_0 v + \frac{\partial P_p}{\partial y} - \frac{E_5}{a_3} V = 0 \quad (35)$$

$$S \frac{\partial^2 v}{\partial t^2} - \frac{\eta}{\gamma} \frac{\partial^2 v}{\partial y^2} + \Omega \sigma_0 \frac{\partial v}{\partial t} - \frac{F_6}{a_3 \omega} \frac{\partial v}{\partial t} = 0 \quad (36)$$

$$P_p - P - \mathcal{L}_7\left(\frac{v}{a_3}\right) = 0 \text{ at } y = l \quad (37)$$

$$P_p - P_c - \mathcal{L}_8\left(\frac{v}{a_3}\right) = 0 \text{ at } y = l + b \quad (38)$$

$$v - \frac{\partial \phi}{\partial y} - \mathcal{L}_9\left(\frac{v}{a_3}\right) + \mathcal{L}_{10}\left(\frac{v}{a_3}\right) = 0 \text{ at } y = l \quad (39)$$

$$v - \frac{\partial \Phi}{\partial y} - \mathcal{L}_{11}\left(\frac{v}{a_3}\right) + \mathcal{L}_{12}\left(\frac{v}{a_3}\right) = 0 \text{ at } y = l + b \quad (40)$$

The solutions of the equivalent linear system subject to the boundary conditions (16) and (17) are of the forms

$$\phi = A \cos \kappa_y e^{i\theta - \alpha x} + CC \quad (41)$$

$$\Phi = B \cos[\omega \kappa_c (y - l - b - h)] e^{i\theta - \alpha x} + CC \quad (42)$$

$$v = C \cos[\kappa_p (y + \Psi)] e^{i\theta - \alpha x} + CC \quad (43)$$

where

$$\kappa^2 = \omega^2 - k^2 - (1/a_1)(E_1 - iF_1) \quad (44)$$

$$\kappa_c^2 = 1 - (1/a_2 \omega^2)(E_3 - iF_3) \quad (45)$$

$$\kappa_p^2 = \kappa_{p0}^2 - \frac{i\gamma}{na_3} F_6 = \frac{\gamma\omega}{n} \left[ \omega S + i\Omega \left( \sigma_0 + \frac{8\sigma_1}{3\pi} a_3 \right) \right] \quad (46)$$

The dispersive equations (44-46) show the crucial nonlinear characteristics of the dependence of dispersion relation on acoustic pressure. Substituting Eqs. (41-43) into Eqs. (32), (34), and (35) gives the expressions for the pressure as

$$P = \frac{1}{\gamma} + \left( i\omega + \frac{E_2}{a_1} - \frac{iF_2}{a_1} \right) A \cos \kappa_y e^{i\theta - \alpha x} + CC \quad (47)$$

$$P_c = \frac{1}{\gamma} + \left( i\omega + \frac{E_4}{a_2} - \frac{iF_4}{a_2} \right) B \cos[\omega \kappa_c (y - l - b - h)] e^{i\theta - \alpha x} \quad (48)$$

$$P_p = \frac{1}{\gamma} + i \frac{n\kappa_p}{\Omega\gamma\omega} C \sin[\kappa_p (y + \Psi)] e^{i\theta - \alpha x} + CC \quad (49)$$

Substituting Eqs. (41-49) into the boundary conditions (37-40) and eliminating the complex amplitude  $A$ ,  $B$ , and  $C$  give the transcendental equation as

$$\kappa \tan \kappa = -i\omega (G_2/Z) \quad (50)$$

where

$$-iZ = \frac{G_1 \cot \omega \kappa_c h - \frac{\eta \kappa_p}{\Omega \gamma \omega} \tan \kappa_p b + i\epsilon_2}{1 + \frac{\Omega \gamma \omega}{n \kappa_p} (G_1 \cot \omega \kappa_c h + i\epsilon_2) \tan \kappa_p b} + \epsilon_1 \quad (51)$$

$G_1$ ,  $G_2$ ,  $\epsilon_1$ , and  $\epsilon_2$  are defined in the Appendix.

Equation (46) shows that the nonlinear collection for resistivity  $8\sigma_1 a_3 / 3\pi$  is similar to those presented by Sirignano,<sup>15</sup> Zinn,<sup>16</sup> and Melling.<sup>17</sup>

For the Helmholtz-type impedance, the equivalent Melling's expression for  $\sigma_1$  is:

$$\sigma_1 = \frac{1 - \Omega^2}{2bC_D^2 \Omega^2} \left( 1 + \frac{1}{r_0} \sqrt{\frac{2\nu}{\omega}} + \frac{16r_0}{3\pi b \Psi'(\Omega^{1/2})} \right) \quad (52)$$

where  $C_D$  is the discharging coefficient of the orifice,  $r_0$  is the hole radius,  $b$  is the physical thickness of porous sheet,  $\nu$  is the kinematic viscosity, and  $\Psi'(\Omega)$  is the Fok function. For duct lining, 22.8% perforated plate with  $b^* = 0.0381$  cm,  $r_0^* = 0.0991$  cm,  $\nu^* = 0.199 \times 10^{-4}$  m<sup>2</sup>/s,  $C_D = 0.86$ , the values of  $\sigma_l$  given by Eq. (52) are 2323 and 2241 for  $f = 1$  and 7 kHz, respectively. The Kurze and Allen<sup>2</sup> experimental data for  $\sigma_l$  corresponding the lining mentioned above is 2293.

In order to identify the nonlinear effect on the attenuation, we separate the eigenvalue  $\kappa$  into two parts and rewrite Eq. (50) as

$$(\kappa_0 + a_1 \kappa_1) \tan(\kappa_0 + a_1 \kappa_1) = -\omega i \frac{1 + f_2(a_1)}{Z_0 + Z_1(a_1)} \quad (53)$$

where  $\kappa_0$  and  $Z_0$  are independent of acoustic pressure, and the term  $a_1 \kappa_1$  is associated with the nonlinear effect of  $f_2(a_1)$  and  $Z_1(a_1)$  on  $\kappa$ . Letting  $A = a(x, t) \exp[\alpha x + i\beta(x, t)]$  with real  $a$  and  $\beta$ , we obtain

$$\frac{\partial a}{\partial x} = -a\alpha + \text{real} \left( k \frac{dA}{d\theta} e^{-\alpha x - i\beta} \right) = -(\alpha_0 + \alpha_1 a - \alpha_2 a^2) a \quad (54)$$

where

$$\alpha = \text{Im}(k_0 + a k_1) = \alpha_0 + \alpha_1 a \quad (55)$$

$$k \frac{dA}{d\theta} = \frac{k M_1}{i(k^2 + \bar{k}^2 - 2\omega^2) \cos \kappa y} \equiv (\alpha_2 + i k_2) A^2 \bar{A} e^{-2\alpha x} \quad (56)$$

The term  $a k_1$  associated with the nonlinear effect must satisfy Eq. (44); i.e.,

$$a^2 k_1^2 + 2a k_0 k_1 + 2a_1 k_0 k_1 + a_1^2 k_1^2 + \frac{E_1 - i F_1}{a_1} = 0 \quad (57)$$

The velocity amplitude at  $y = 1$  and the sound pressure level are related to  $a_1$  or  $a$  by

$$a = \frac{|\partial \phi / \partial y|_{y=1}}{2 |\kappa \sin \kappa|} = \frac{|v|_{y=1}}{2 |\kappa \sin \kappa|} = \frac{a_1}{2 |\cos \kappa|} \quad (58)$$

and

$$\frac{dL}{dx} = -8.7(\alpha_0 + \alpha_1 a - \alpha_2 a^2) \quad (59)$$

#### IV. Numerical Results

Very good agreement between the present analytical results and the experimental data of Kurze and Allen<sup>2</sup> is obtained for the propagation of the lowest mode in a lined duct. Figure 1 shows that the absorption vs frequency curve is flatter for a higher sound pressure level. The ratio of the nonlinear collection  $8\sigma_l a_3 / 3\pi$  to the linear resistivity  $\sigma_0$  for SPL 160 dB is 0.6, and it indicates that the recreated fundamental harmonic due to the material nonlinearity is not negligible for the calculation of the eigenvalue in Eq. (50). Note that only three of  $b$ ,  $\Omega$ ,  $\rho_e$ ,  $s$ , and  $\sigma_0$  are independent parameters. In order to comply with the increase in the air density inside the porous medium, the experimental data for the effective density and the linear resistivity are suggested to be used.

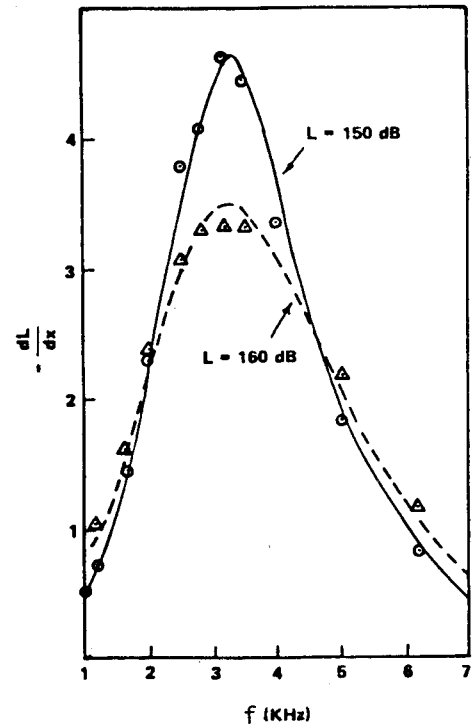


Fig. 1 Comparison of the present analytical results with the experimental data of Kurze and Allen (1971) for the lowest mode,  $d^* = 2.54$  cm,  $b^* = 0.0381$  cm,  $h^* = 1.905$  cm,  $\Omega = 0.95$ ,  $s = 1.15$ ,  $\sigma_0 = 53.33$ , and  $\sigma_l = 2293$ .

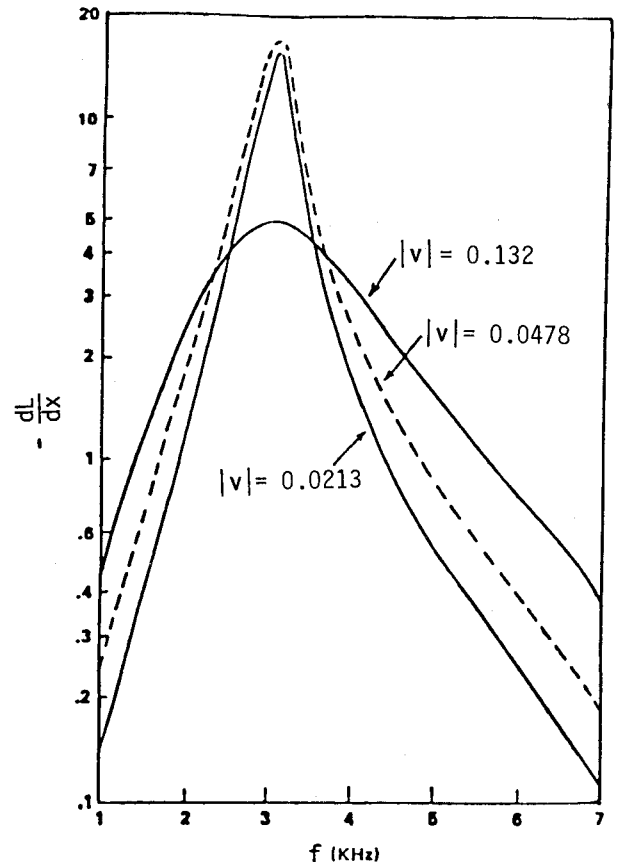


Fig. 2 Comparisons at absorption coefficients at various particle velocities,  $\sigma_0 = 7.64$ ,  $d = 2.54$  cm,  $\sigma_l = 466$ ,  $b = 0.0381$  cm,  $\Omega = 0.6$ ,  $s = 4.3$ ,  $h = 1.905$  cm

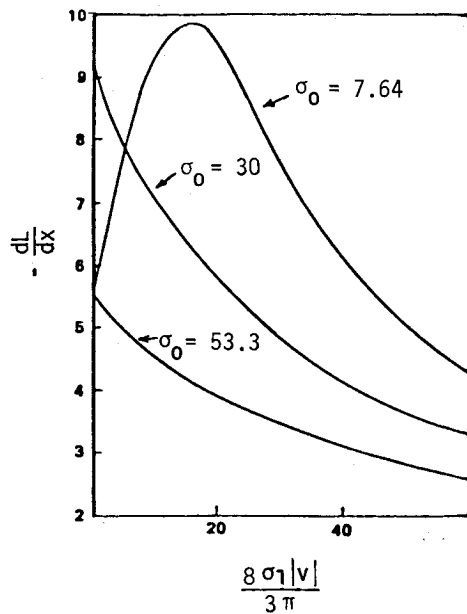


Fig. 3 Variations of absorption coefficients with increasing nonlinear resistivity at  $f=3$  kHz,  $\Omega=0.95$ ,  $s=1.15$ ,  $b=0.0381$  cm,  $d=2.54$  cm,  $h=1.905$  cm.

Figure 2 shows that the nonlinearities increase the attenuation for all frequencies when the SPL start increasing, and then the absorption vs frequency curve becomes flatter with further increasing SPL. Thus, whenever the linear resistivity is very low, the nonlinearity effects are favorable for a very wide range of frequencies.

Figure 3 illustrates the variations of the absorption with increasing SPL. For  $\sigma_0=7.64$ , it shows that there is a maximum attenuation rate at a certain value of SPL for the frequency near resonance. However, when the linear resistivity is high, the nonlinear effect always decreases the attenuation for those frequencies near resonance.

According to Eq. (59), the positive value of  $(\alpha_1 a - \alpha_2 a^2)$  corresponds to the favorable nonlinear effect on attenuation while the negative one corresponds to the adverse nonlinear effect. The term  $\alpha_2 a^2$  is contributed entirely by the gas nonlinearity and has been shown<sup>13</sup> to be much smaller than  $\alpha_1 a$  for a lining material such as porous face-sheet. Except for the lining material with weak nonlinear behavior such as fibrous metal, the  $\alpha_2 a^2$  term in Eq. (59) can be neglected for the determination of the nonlinear effect on the attenuation. Tables 1 and 2 show that whenever the product of the linear

resistivity and the thickness of the porous sheet are smaller, the bandwidth of the adverse nonlinear effect will become narrower and the frequencies corresponding to this bandwidth will shift to higher values.

Table 1 Variations of the coefficients of nonlinear attenuation term with frequency  $\omega$ ,  $\sigma_0=50$ ,  $\sigma_1=1000$ ,  $h=0.508$  cm,  $\Omega=0.95$ ,  $|v|=0.01$ ,  $S=1.15$

| $\alpha_1 = \left( \alpha_0 - \frac{I}{8.7} \frac{dL}{dx} \right) / a$ |               |               |               |
|--|---------------|---------------|---------------|
| $\omega$   | $b=0.0381$ cm | $b=0.0635$ cm | $b=0.0889$ cm |
| 1.0  | 0.1294        | 0.1969        | 0.2256        |
| 2.0  | 3.244         | 1.503         | -0.7531       |
| 2.5  | 8.275         | -4.125        | -7.898        |
| 3.0  | 2.419         | -33.97        | -22.06        |
| 3.5  | -97.68        | -107.5        | -32.91        |
| 4.0  | -478.0        | -1.368        | -23.10        |
| 4.5  | -2327.0       | 11.74         | -4.347        |
| 5.0  | 6.325         | 8.401         | 3.546         |
| 6.0  | 3.281         | 4.831         | 5.164         |
| 7.0  | 2.066         | 3.207         | 4.133         |
| 8.0  | 1.437         | 2.318         | 3.242         |
| 9.0  | 1.063         | 1.771         | 2.615         |
| 10.0   | 0.8176        | 1.409         | 2.184         |

Table 2 Variation of the coefficients of nonlinear attenuation term with frequency  $\omega$ ,  $b=0.0381$  cm,  $\sigma_1=1000$ ,  $h=0.508$  cm,  $\Omega=0.95$ ,  $S=1.15$ ,  $|v|=0.01$

| $\alpha_1 = \left( \alpha_0 - \frac{I}{8.7} \frac{dL}{dx} \right) / a$ |                     |                |
|--|---------------------|----------------|
| $\omega$   | $\sigma_0=20$       | $\sigma_0=100$ |
| 1.0  | 0.1407              | 0.09772        |
| 2.0  | 5.648               | 0.3603         |
|  | 2.529.33            | -2.250         |
| 3.0  | 164.4               | -11.21         |
| 3.5  | 1064.0              | -25.23         |
| 4.0  | 7574.0              | -21.25         |
| 5.0  | $3996 \times 10^2$  | 3.331          |
| 5.5  | $-3703 \times 10^2$ | 3.121          |
| 6.0  | $-4256 \times 10^5$ | 2.614          |
| 7.0  | 2.096               | 1.825          |
| 8.0  | 1.455               | 1.333          |
| 9.0  | 1.072               | 1.014          |
| 10.0   | 0.8225              | 0.7941         |

## Appendix

$$\frac{M_1}{A^2 \bar{A} e^{-2\alpha x}} = \left[ \frac{\gamma-1}{2} \omega^2 (k^2 - 2|k|^2) + |k|^2 (|k|^2 - 2k^2) \right] |\cos \kappa y|^2 \cos \kappa y - \left[ \frac{\gamma-1}{2} \omega^2 \kappa^2 + |k|^4 - 2|k|^2 \kappa^2 \right] \cos \kappa y \sin^2 \kappa y$$

$$- [(\gamma-1) \omega^2 |k|^2 + 2|k|^2 \kappa^2] \cos \kappa y |\sin \kappa y|^2$$

$$\frac{M_2}{A^2 \bar{A} e^{-2\alpha x}} = \frac{i}{2} \omega [\omega^2 (2-\gamma) - k^2 - 2|k|^2] |\cos \kappa y|^2 \cos \kappa y + \frac{i}{2} \omega \kappa^2 \sin^2 \kappa y \cos \kappa y - i \omega |k|^2 \cos \kappa y |\sin \kappa y|^2$$

$$\frac{M_3}{B^2 \bar{B} e^{-2\alpha x}} = - \left( \frac{\gamma-1}{2} \omega^2 \kappa^2 + |k|^4 \right) \cos \kappa y \sin^2 \kappa y - [(\gamma-1) \omega^2 + 2\kappa^2] |k|^2 \cos \kappa y |\sin \kappa y|^2$$

$$\frac{M_4}{B^2 \bar{B} e^{-2\alpha x}} = \frac{i}{2} \omega^3 (2-\gamma) |\cos \kappa y|^2 \cos \kappa y + \frac{i}{2} \omega \kappa^2 \sin \kappa y \cos \kappa y - i \omega |k|^2 \cos \kappa y |\sin \kappa y|^2$$

$$M_5 = -\frac{4a_3^2}{3\pi} \sigma_1 e^{i\tau_3 - \alpha x} = -\frac{16}{3\pi} \sigma_1 |C|^2 |\cos \kappa_p (y + \Psi)|^2 e^{i\tau_3 - \alpha x}$$

$$M_6 = \frac{i4}{3\pi} \omega \Omega \sigma_1 a_3^2 e^{i\tau_3 - \alpha x}$$

$$\frac{M_7}{e^{-2\alpha x}} = \frac{-i}{2\omega} \left[ \bar{A} C^2 \bar{k}^2 \left( 1 - \frac{E_2}{i\omega a_1} - \frac{F_2}{\omega a_1} \right) \cos^2 [\kappa_p (I + \Psi)] \cos \bar{k} + 2A |C|^2 k^2 \cdot \left( 1 + \frac{E_2}{i\omega a_1} - \frac{F_2}{\omega a_1} \right) \cos \kappa |\cos \kappa_p (I + \Psi)|^2 \right] \\ + \frac{i\eta}{2\Omega \gamma \omega^3} |C|^2 C [2\kappa_p^3 |\cos \kappa_p (I + \Psi)|^2 \sin [\kappa_p (I + \Psi)] + \bar{\kappa}_p^3 \cos^2 [\kappa_p (I + \Psi)] \sin [\bar{\kappa}_p (I + \Psi)]]$$

$$\frac{M_8}{e^{-2\alpha x}} = \frac{-i}{2\omega} \left[ \bar{B} C^2 \omega^2 \left( 1 - \frac{E_4}{i\omega a_2} - \frac{F_4}{\omega a_2} \right) \bar{\kappa}_c^2 \cos^2 [\kappa_p (I + b + \psi)] \cos \omega \bar{\kappa}_c h \right. \\ \left. + 2|B| C^2 \omega^2 \kappa_c^2 \left( 1 + \frac{E_4}{i\omega a_2} - \frac{F_4}{\omega a_2} \right) |\cos \kappa_p (I + b + \Psi)|^2 \cos \omega \kappa_c h \right] \\ + \frac{in}{2\Omega \gamma \omega} |C|^2 C [2\kappa_p^3 |\cos \kappa_p (I + b + \Psi)|^2 \sin [\kappa_p (I + b + \Psi)] + \bar{\kappa}_p^3 \cos^2 [\kappa_p (I + b + \Psi)] \cdot \sin [\bar{\kappa}_p (I + b + \Psi)]]$$

$$\frac{M_9}{e^{-2\alpha x}} = \frac{-I}{2\omega^2} [C^2 \bar{A} \bar{k}^3 \sin \bar{k} \cos^2 [\kappa_p (I + \Psi)] - 2A |C|^2 \kappa^3 \sin \kappa |\cos \kappa_p (I + \Psi)|^2] \\ - \frac{I}{\omega^2} [\bar{A} C^2 \bar{k} |k|^2 \sin \bar{k} \cos^2 \kappa_p (I + \Psi) - A |C|^2 \kappa k (\bar{k} - k) \sin \kappa |\cos \kappa_p (I + \Psi)|^2]$$

$$\frac{M_{10}}{e^{-2\alpha x}} = \frac{|C|^2 C}{2\omega^2} \cos |\kappa_p (I + \Psi)|^2 \cos [\kappa_p (I + \Psi)] (\bar{\kappa}_p^2 - 2\kappa_p)$$

$$\frac{M_{11}}{e^{-2\alpha x}} = \frac{\omega}{2} [C^2 \bar{B} \bar{\kappa}_c^3 \cos^2 [\kappa_p (I + b + \Psi)] \sin \omega \bar{\kappa}_c h - 2|C|^2 \kappa_c^3 |\cos \kappa_p (I + b + \Psi)|^2 \cdot \sin \omega \kappa_c h]$$

$$\frac{M_{12}}{e^{-2\alpha x}} = \frac{|C|^2 C}{2\omega^2} (\bar{\kappa}_p^2 - 2\kappa_p) |\cos \kappa_p (I + b + \Psi)|^2 \cos \kappa_p [(I + b + \Psi)]$$

$$G_{1\kappa_c} = \left( 1 + \frac{E_4}{ia_2\omega} - \frac{F_4}{a_2\omega} \right) (I + \epsilon_{11} - \epsilon_{12})$$

$$G_2 = \left( 1 + \frac{E_2}{i\omega a_1} - \frac{F_2}{\omega a_1} \right) (I + \epsilon_9 - \epsilon_{10}), \quad \epsilon_n = -\frac{E_n}{a_3} + \frac{iF_n}{a_3}$$

## References

- <sup>1</sup>Ingard, U., "Nonlinear Attenuation of Sound in a Duct," *Journal of the Acoustical Society of America*, Vol. 43, 1968, pp. 167-168.
- <sup>2</sup>Kurze, U. J. and Allen, C. H., "Influence of Flow and High Sound Level on the Attenuation in a Lined Duct," *Journal of the Acoustical Society of America*, Vol. 49, 1971, pp. 1643-1653.
- <sup>3</sup>Nayfeh, A. H. and Tsai, M. S., "Nonlinear Acoustic Propagation in Two-Dimensional Ducts," *Journal of the Acoustical Society of America*, Vol. 55, 1974, pp. 1166-1172.
- <sup>4</sup>Nayfeh, A. H. and Tsai, M. S., "Finite Amplitude Waves in Two-Dimensional Lined Ducts," *Journal of Sound and Vibration*, Vol. 37, 1974, pp. 27-38.
- <sup>5</sup>Krylov, N. and Bogoliubov, N. N., *Introduction to Nonlinear Mechanics*, Princeton University Press, Princeton, N.J., 1947.
- <sup>6</sup>Bogoliubov, N. N. and Mitropolski, Y. A., *Asymptotic Methods in the Theory of Nonlinear Oscillations*, Gordon and Breach, New York, 1961.
- <sup>7</sup>Green, L. and Dawez, P., "Fluid Flow Through Porous Metals," *Journal of Applied Mechanics*, Vol. 18, 1951, pp. 39-45.
- <sup>8</sup>Irmay, S., "On the Theoretical Derivation of Darcy and Forchheimer Formula," *American Geophysical Union Transactions*, Vol. 39, 1958, pp. 702-707.
- <sup>9</sup>Morse, P. M. and Ingard, U., *Theoretical Acoustics*, McGraw-Hill Book Co., Inc., New York, 1968.
- <sup>10</sup>Zwikker, C. and Kosten, C. W., *Sound Absorbing Material*, Elsevier Publishing Co., New York, 1947.
- <sup>11</sup>Dean, P. D., "An in Situ Method of Wall Acoustic Impedance Measurement in Flow Ducts," *Journal of Sound and Vibration*, Vol. 34, 1974, pp. 97-130.
- <sup>12</sup>Hersh, A. S. and Walker, B., "Effects of Grazing Flow on the Steady-State Flow Resistance and Acoustic Impedance of Thin Porous-Faced Liners," AIAA Paper 77-1335, Oct. 1977.
- <sup>13</sup>Tsai, M. S., "High Intensity Sound in Lined Ducts," Ph.D. Thesis, Virginia Polytechnic Institute, March 1974.
- <sup>14</sup>Van der Pol, B., "On Oscillation Hysteresis in a Simple Triode Generator," *Philosophic Magazine*, Vol. 43, 1926, pp. 700-719.
- <sup>15</sup>Sirignano, W. A., "Nonlinear Dissipation in Acoustic Liner," AMS Rept. No. 553-f, Princeton Univ., 1966, p. 31.
- <sup>16</sup>Zinn, B. T., "A Theoretical Study of Non-linear Damping by Helmholtz Resonators," *Journal of Sound and Vibration*, Vol. 13, 1970, pp. 347-356.
- <sup>17</sup>Melling, T. H., "The Acoustic Impedance of Perforates at Medium and High Sound Pressure Levels," *Journal of Sound and Vibration*, Vol. 29, 1973, pp. 1-65.